NATIONAL ADVISORY COMMITTEE FOR AERONAUTICS

TECHNICAL NOTE 1973

THEORETICAL SPANWISE LIFT DISTRIBUTIONS OF LOW-ASPECT-RATIO WINGS AT SPEEDS BELOW AND ABOVE THE SPEED OF SOUND

By Franklin W. Diederich and Martin Zlotnick

Langley Aeronautical Laboratory
Langley Air Force Base, Va.

Washington
October 1949

NATIONAL ADVISORY COMMITTEE FOR AERONAUTICS

TECHNICAL NOTE 1973

THEORETICAL SPANWISE LIFT DISTRIBUTIONS OF LOW-ASPECT-RATIO WINGS AT SPEEDS BELOW AND ABOVE THE SPEED OF SOUND

By Franklin W. Diederich and Martin Zlotnick

SUMMARY

The spanwise lift distributions of wings of low aspect ratio but of arbitrary plan form and angle-of-attack distribution have been analyzed by two well-established concepts: the virtual-mass concept and the Weissinger method. Both concepts have been found to yield the same simple integral expression for the spanwise lift distribution in terms of the spanwise angle-of-attack distribution. Tables and figures of lift distributions of low-aspect-ratio wings have been presented. Within certain limitations these distributions are independent of the plan form. For plan forms with leading edges swept back behind the Mach cone, the results of the analysis are applicable at supersonic speeds.

INTRODUCTION

For wings of very low aspect ratio, of the order of 1 or less, at small angles of attack the flow may be assumed to be esentially two-dimensional in planes normal to the stream direction. (See reference 1.) In the present paper this concept is shown to lead to a simple formulation of the problem of calculating the spanwise lift distribution of wings of very low aspect ratio for various angle-of-attack distributions in terms of conditions at the widest section of the wing. The same problem is also formulated as a limiting case of the Weissinger L-method. (See reference 2.) Some comparisons are drawn between the assumptions and limitations of the two approaches.

Spanwise lift distributions have been calculated for angle-of-attack distributions which correspond to several symmetrical and antisymmetrical twists, as well as to the deflection of flaps and ailerons of various spans. The results are presented in a table and in several figures.

SYMBOLS

A	aspect ratio
b	wing span (at widest section)
b_a	aileron span (total for both wings)
b_f	flap span (total for both wings)
c	chord
c^*	dimensionless chord $\left(\frac{c}{b/2}\right)$
$\bar{c}$	average chord $\left(\frac{S}{b}\right)$
c_l	local lift coefficient
C_L	wing lift coefficient $\left(\frac{L}{qS}\right)$
$C_{L_{l/2}}$	lift coefficient on either half of wing $\left(\frac{L_{l/2}}{qS/2}\right)$
C_{D_i}	induced drag coefficient
C_l	rolling-moment coefficient $\left(\frac{\text{Rolling moment}}{qSb}\right)$
C_{BM}	bending-moment coefficient $\left(\frac{\text{Bending moment}}{q(S/2)(b/2)}\right)$
L	lift
$L_{l/2}$	lift on either half of wing
M	vertical momentum of virtual mass per unit length
q	dynamic pressure
S	wing area
V	airspeed
w	downwash velocity

y	spanwise distance
y^*	dimensionless spanwise distance (fraction of semispan)
$\bar{y}^*$	dimensionless spanwise distance of center of pressure (fraction of semispan)
y_o^*	dimensionless spanwise distance at point of discontinuity in angle of attack
α	angle of attack (slope of mean-camber surface), radians
α_t	angle of attack at tip, radians
α_δ	flap or aileron effectiveness parameter $\left(\frac{\partial c_l/\partial\delta}{\partial c_l/\partial\alpha}\right)$
Γ	circulation
Γ^*	dimensionless circulation $\left(\frac{4\Gamma}{bV}$ or $c^*c_l\right)$
γ	loading coefficient $\left(\frac{c_l c}{\bar{c}}$ or $\frac{A}{2}\Gamma^*\right)$
δ	flap or aileron deflection, radians
η^*	variable of integration corresponding to y^*
θ	trigonometric variable corresponding to $y^*(\cos^{-1} y^*)$
ϑ	variable of integration corresponding to θ
Λ	sweep angle

ANALYSIS

The Virtual-Mass Approach

According to the theory of reference 1 the disturbance set up by wings of low aspect ratio at small angles of attack is essentially two-dimensional in planes perpendicular to the free stream. The lift on a spanwise strip of width dx may then be obtained from the time rate of

change of the vertical momentum of the virtual mass associated with the given two-dimensional flow

$$dL = \frac{dM}{dt}\,dx$$

$$= V\frac{dM}{dx}\,dx$$

$$= V\,dM$$

where M is the vertical momentum of the virtual mass per unit length. The lift on the entire wing is then

$$L = V\,M_{b_{max}} \tag{1}$$

where $M_{b_{max}}$ is the downward vertical momentum at the maximum width of the airfoil. Any portion of the wing behind the section of maximum width is assumed to be alined with the wake so that it does not affect the lift.

Equation (1) indicates that the lift depends entirely on the geometry of the widest section. A physical interpretation of this equation is that the wake leaves the airfoil parallel to the surface at the section of maximum width and that the vorticity distribution in the wake is such as to produce the required downwash distribution in any plane perpendicular to the wake. The determination of the spanwise lift distribution on the wing then reduces to a problem almost identical in form with that of two-dimensional thin-airfoil theory and very similar to but simpler than the classical lifting-line theory.

If the bound circulation on the wing at any spanwise location is given by the parameter

$$\gamma = \frac{A}{Vb/2}\Gamma$$

and if the spanwise distance is given by the parameter

$$y^* = \frac{y}{b/2}$$

and an associated variable of integration η^*, then the downwash angle at any spanwise location y^* in the wake is given by

$$\frac{w}{V} = \frac{1}{2\pi A}\int_{-1}^{1} \frac{d\gamma}{d\eta^*}\frac{d\eta^*}{y^* - \eta^*} \tag{2}$$

From the foregoing considerations this angle must be equal to α, the slope of the mean-camber surface at the widest section. If, furthermore, the trigonometrical variables θ and ϑ are defined as

$$\theta = \cos^{-1} y^*$$

$$\vartheta = \cos^{-1} \eta^*$$

equation (2) becomes

$$\frac{1}{2\pi A}\int_{0}^{\pi} \frac{d\gamma}{d\vartheta}\frac{d\vartheta}{\cos\vartheta - \cos\theta} = \alpha \tag{3}$$

Equation (3) may be solved by means of an inversion integral:

$$\gamma = \frac{2}{\pi}A\int_{0}^{\pi} \alpha \sin\vartheta \log\frac{\sin\frac{\vartheta+\theta}{2}}{\sin\frac{|\vartheta-\theta|}{2}}\,d\vartheta \tag{4}$$

For a constant angle of attack, for instance, equation (4) yields an elliptic lift distribution with a lift coefficient equal to $\frac{\pi}{2}A\alpha$ in agreement with the result of reference 1.

Three-Quarter-Chord Approach

Another approach to the problem of calculating spanwise lift distributions on wings of low aspect ratio is to consider the limit, as the aspect ratio goes to zero, of the equations of the Weissinger L-method. This method consists of concentrating the bound vorticity at the quarter-chord line, calculating the downwash angle at the three-quarter-chord

line, and setting that downwash angle equal to the slope of the mean-camber surface at the three-quarter-chord line. This equation may be written as

$$\frac{1}{4\pi}\int_{-1}^{1}\frac{d\Gamma^*}{d\eta^*}\frac{d\eta^*}{y^*-\eta^*}+\frac{1}{8\pi}\frac{1}{c^*/2}\int_{-1}^{1}F(y^*,\eta^*)\frac{d\Gamma^*}{d\eta^*}\,d\eta^*=\alpha \qquad (5)$$

where the dimensionless circulation Γ^* is defined as

$$\Gamma^*=\frac{4\Gamma}{bV}$$

and the plan-form function F is defined, for $\eta^* \geqq 0$, as

$$F=\frac{c^*/2}{y^*-\eta^*}\left\{\sqrt{\left[1+\left(\frac{y^*-\eta^*}{c^*/2}\right)\tan\Lambda\right]^2+\left(\frac{y^*-\eta^*}{c^*/2}\right)^2}-1\right\}$$

and, for $\eta^* \leqq 0$, as

$$F=\frac{c^*/2}{y^*-\eta^*}\left\{\frac{\sqrt{\left[1+\left(\frac{y^*+\eta^*}{c^*/2}\right)\tan\Lambda\right]^2+\left(\frac{y^*-\eta^*}{c^*/2}\right)^2}}{1+2\frac{y^*}{c^*/2}\tan\Lambda}-1\right\}$$

$$+2\tan\Lambda\,\frac{\sqrt{\left(1+\frac{y^*}{c^*/2}\tan\Lambda\right)^2+\left(\frac{y^*}{c^*/2}\right)^2}}{1+2\frac{y^*}{c^*/2}\tan\Lambda}$$

and where α now represents the slope of the mean-camber surface at the three-quarter-chord line.

As the aspect ratio approaches zero, the F function approaches the value $\tan\Lambda$, which is constant if the semispan quarter-chord line is straight. For instance, all plan forms of figure 1 except that of figure 1(c) have straight quarter-chord lines. If F is constant the second integral in equation (5) vanishes. Furthermore, the dimensionless chord c^* approaches infinity and its reciprocal vanishes. Consequently, the second term of equation (5) may be expected to approach zero quite rapidly as the aspect ratio approaches zero.

If the parameter γ, which is related to the dimensionless circulation Γ^* by

$$\gamma = \frac{A\Gamma^*}{2}$$

and the trigonometric variables are substituted in equation (5) and if the second term is neglected, equation (5) becomes identical with equation (3), except that α now stands for the angle of attack at the three-quarter-chord line. The solution for the circulation is then given by equation (4) as before.

RESULTS

In order to facilitate the application of equation (4) to cases of practical interest, the integral of that equation has been evaluated for several angle-of-attack distributions which can be expressed analytically as follows:

(a) The constant angle-of-attack or additional-loading case analyzed in reference 1

(b) The linear antisymmetrical-twist or damping-in-roll case previously analyzed in reference 3

(c) The symmetrical- and antisymmetrical-twist-distribution cases $\alpha = \alpha_t |y^*|^n$ in which α_t is the angle of attack at the tip and is considered to have equal and opposite values at the two tips in the antisymmetrical case

(d) The flap case in which $\alpha = \alpha_\delta \delta$ from $y^* = -y_o^*$ to $y^* = y_o^*$ and $\alpha = 0$ elsewhere, $\alpha_\delta \delta$ being the effective angle of attack due to flap deflection (some considerations involved in the selection of the value of α_δ are outlined in the section entitled "Discussion")

(e) The aileron case in which $\alpha = \pm\alpha_\delta \delta$ outboard of $y^* = \pm y_o^*$ and $\alpha = 0$ elsewhere

The resulting lift distributions for cases (a) to (e) are presented in table 1 and in figures 2 to 5. All results are presented for unit aspect ratio A and unit angle of attack α, where α is the angle of attack at the tip for the twist cases and is the effective angle of attack due to control deflection $\alpha_\delta \delta$ for the flap and aileron cases.

The twist distributions of case (c) may be useful in the analysis of structural twists. If a structural twist distribution is of the type considered in case (c), the corresponding lift distribution may be taken from the table or the figures directly. Otherwise, a structural twist distribution can usually be approximated by the linear superposition of two or more of the twist distributions covered in case (c). The lift distribution is then given by a superposition of the lift distributions corresponding to those particular twist distributions.

The results for case (d) may be applied to the case of symmetrically deflected ailerons by subtracting a flap distribution from the constant-angle-of-attack distribution for the same angle. Similarly, the results for case (e) may be used to calculate the lift distribution due to inboard ailerons by subtracting the aileron distribution for the given value of y_o* from the aileron distribution for 100-percent-semispan aileron.

From the lift distributions the lift, rolling, and bending moments, as well as the lateral center of pressure of the wing, may be calculated in the form of dimensionless coefficients:

$$C_L = \frac{1}{2}\int_0^{\pi} \gamma \sin\theta \, d\theta$$

$$C_{L_{1/2}} = \int_0^{\pi/2} \gamma \sin\theta \, d\theta$$

$$C_l = \frac{1}{8}\int_0^{\pi} \gamma \sin 2\theta \, d\theta$$

$$C_{BM} = \frac{1}{2}\int_0^{\pi/2} \gamma \sin 2\theta \, d\theta$$

$$\bar{y}* = \frac{C_{BM}}{C_{L_{1/2}}}$$

The values of these coefficients for the various angle-of-attack distributions are given in table 1; the lift coefficient due to flap deflection and the rolling moment due to aileron deflection are also given in figure 6 as functions of the flap or aileron span ratio.

The induced drag coefficient may be calculated from the conventional lifting-line equation since the drag is not affected by the longitudinal distribution of the lift. Consequently,

$$C_{D_i} = \frac{1}{4}\int_0^{\pi} \alpha\gamma \sin\theta \, d\theta \tag{6}$$

For the constant angle-of-attack case equation (6) becomes

$$C_{D_i} = \frac{C_L^2}{\pi A}$$

as also given in reference 1.

DISCUSSION

The two approaches to the problem of calculating the spanwise lift distributions of wings of low aspect ratio presented in this paper have in common all the limitations of linear potential theory and are subject to certain additional inherent limitations as well. These additional limitations and the effect they have on the validity of the results of the two approaches are discussed in the succeeding paragraphs.

The validity of the virtual-mass approach has been demonstrated for the constant-angle-of-attack case in references 1 and 4 and for the linear antisymmetric angle-of-attack case in reference 5 primarily by comparison with more rigorous analytical methods. The validity of the Weissinger L-method for plan forms of low aspect ratios has similarly been demonstrated for the constant-angle-of-attack case in references 2 and 4 and for the linear antisymmetric case in reference 5 by comparison with both analytical and experimental results. The extension of the approach of reference 1 and the specialization of the method of reference 2 presented in this paper may therefore also be expected to be valid provided certain conditions of aspect ratio, plan form, angle of attack, and Mach number are met.

The aspect ratio has been assumed to be vanishingly small in the analysis. For the purpose of comparison the lift-curve slopes and

additional lift distributions calculated by the method of reference 2 are shown in figure 7 for various plan forms of aspect ratio 1.5 together with the values calculated by the low-aspect-ratio analysis of the present paper, namely an elliptic lift distribution and a lift-curve slope of $\frac{\pi}{2}(1.5) = 2.356$. At an aspect ratio of 1.5 the lift distributions for the various plan forms are in fair agreement with the elliptic distribution and with each other. The lift-curve slopes of the various plan forms are almost the same and are about 15 percent lower on the average than that calculated by the simplified analysis. This type of agreement does not appear to be sufficient for most practical purposes. In reference 1, however, the lift-curve slope is shown to be overestimated by only about 4 percent at an aspect ratio of 1 as compared with a more exact lifting-surface method. Consequently, an aspect ratio of 1 may in general be regarded as the upper limit at which the results of the analysis of this paper may be expected to apply.

The virtual-mass concept utilized in reference 1 does not imply any plan-form or angle-of-attack restrictions except that the aspect ratio must be low and that there cannot be any abrupt longitudinal changes in the span or the slope of the surface. As pointed out in reference 1, however, it is convenient to apply this concept only to pointed plan forms such as those shown in figures 1(b), 1(d), 1(e), 1(f), 1(h), 1(i), and 1(j). Wings with re-entrant trailing edges cannot be conveniently treated by this method. Furthermore, any part of the wing downstream of the widest section must be alined with the widest section. Any flaps and ailerons (such as those shown in fig. 1(h)) must themselves be of low aspect ratio in order for the low-aspect-ratio analysis to apply to the wing.

The Weissinger L-method, on the other hand, applies to all plan forms except those with curved or discontinuous quarter-chord lines or discontinuous chord distributions (it does not, for instance, apply to an elliptic plan form). It has the disadvantage, however, of being strictly applicable only to uncambered wings. This observation results from the following reasoning: The Weissinger method is based on the slope of the mean-camber surface at the three-quarter-chord line at all aspect ratios. For wings of very low aspect ratio the virtual-mass concept indicates that the widest section determines the lift on the wing. Consequently, the application of the Weissinger method to wings of low aspect ratio can give correct results only if the wing is uncambered, so that the slope at the three-quarter-chord line is equal to that at the widest section.

Consequently, the virtual-mass concept is (for practical purposes) more restricted as to plan form but less restricted as to camber than

the three-quarter-chord method. In view of the agreement of the two concepts in the cases to which both apply, however, slight deviations from the plan-form conditions of the one or the camber conditions of the other may be expected to have little effect on the results.

If either concept is used to analyze a wing with deflected flaps or ailerons, the question arises as to what value to choose for the parameter α_δ. According to the virtual-mass concept a particular flap or aileron angle will be just as effective in producing lift as the same angle imposed on the entire section; therefore the parameter α_δ is 1 and the flap or aileron chord ratio does not enter into the problem. On the other hand, the three-quarter-chord concept is applicable only if the flap or aileron occupies 100 percent of the chord, in which case α_δ is again 1. In the more conventional case of partial-chord flaps and ailerons it might be expected, by analogy to the trailing-edge concept, that a value of α_δ between 1 and the two-dimensional value of about 1/2 should be chosen rather than the two-dimensional value for the given flap or aileron chord ratio; the determination of the exact value would require either experimentation or a more refined theory.

The angle of attack has been assumed small in the analysis for several reasons: At large angles of attack the flows in planes perpendicular to the direction of flight cannot be considered to be independent of each other, the trailing vorticity is not shed substantially in the plane of the wing but more nearly parallel to the direction of flight, and, finally, at large angles of attack the flow separates and potential-flow considerations no longer apply.

If the leading edge and the sides of the wing (in the case of plan forms of the type shown in figs. 1(a), 1(b), 1(e), and 1(f), for instance) are sharp the flow may detach at very low angles of attack. The flow separation affects both the total lift, which assumes a parabolic variation with angle of attack rather than the usual linear one, and the lift distribution. (See reference 6.) The theoretical treatment of this phenomenon transcends the scope of this paper; an analysis of a simple case is presented in reference 7. If the leading edge and sides are well rounded, the flow separation and the resulting parabolic variation of the lift coefficient and distortion of the lift distribution tend to be postponed to higher angles of attack. At lower angles of attack the analysis of this paper may be applied to the problem.

The virtual-mass approach has been shown to be valid for supersonic speeds (reference 1), provided the leading edge is swept back sufficiently far behind the Mach cone, as well as for subsonic speeds. Computation of the downwash in the manner utilized in this paper is also valid at supersonic speeds because far downstream of the cross element

of a horseshoe vortex the downwash is the same whether the vortex is in subsonic or supersonic flow. Consequently, the three-quarter-chord concept may also be expected to be valid at supersonic speeds provided the leading edge is swept back far behind the Mach cone and provided the angle-of-attack, camber, and plan-form conditions are such that the analysis of this paper applies.

CONCLUDING REMARKS

The spanwise lift distributions of wings of low aspect ratio but of arbitrary plan form and angle-of-attack distribution have been analyzed by two well-established concepts: the virtual-mass concept and the Weissinger method. Both concepts have been found to yield the same simple integral expression for the spanwise lift distribution in terms of the spanwise angle-of-attack distribution. Tables and figures of lift distributions of low-aspect-ratio wings have been presented. Within certain limitations these distributions are independent of the plan form. For plan forms with leading edges swept back far behind the Mach cone, the results of the analysis are applicable at supersonic speeds.

Langley Aeronautical Laboratory
National Advisory Committee for Aeronautics
Langley Air Force Base, Va., August 25, 1949

REFERENCES

1. Jones, Robert T.: Properties of Low-Aspect-Ratio Pointed Wings at Speeds below and above the Speed of Sound. NACA Rep. 835, 1946.

2. Weissinger, J.: The Lift Distribution of Swept-Back Wings. NACA TM 1120, 1947.

3. Ribner, Herbert S.: The Stability Derivatives of Low-Aspect-Ratio Triangular Wings at Subsonic and Supersonic Speeds. NACA TN 1423, 1947.

4. DeYoung, John: Theoretical Additional Span Loading Characteristics of Wings with Arbitrary Sweep, Aspect Ratio, and Taper Ratio. NACA TN 1491, 1947.

5. Bird, John D.: Some Theoretical Low-Speed Span Loading Characteristics of Swept Wings in Roll and Sideslip. NACA TN 1839, 1949.

6. Winter, H.: Flow Phenomena on Plates and Airfoils of Short Span. NACA TM 798, 1936.

7. Bollay, William: A Non-Linear Wing Theory and Its Application to Rectangular Wings of Small Aspect Ratio. Z.f.a.M.M., Bd. 19, Heft 1, Feb. 1939, pp. 21-35.

TABLE 1.- LIFT DISTRIBUTIONS, LIFT COEFFICIENTS, AND MOMENT COEFFICIENTS FOR VARIOUS ANGLE-OF-ATTACK DISTRIBUTIONS

Angle-of-attack distributions		$\frac{\gamma}{A\alpha}$	$\frac{C_L}{A\alpha}$	$\frac{C_{L_{1/2}}}{A\alpha}$	$\frac{C_l}{A\alpha}$	$\frac{C_{BM}}{A\alpha}$	$\bar{y}^*$
Symmetric	Constant	$2 \sin\theta$	$\frac{\pi}{2}$	$\frac{\pi}{2}$	0	$\frac{2}{3}$	$\frac{4}{3\pi}$
	Linear	$\frac{2}{\pi}\left[\cos^2\theta \log \tan\left(\frac{\pi}{4}+\frac{\theta}{2}\right) + \sin\theta\right]$	$\frac{2}{3}$	$\frac{2}{3}$	0	$\frac{1}{\pi}$	$\frac{3}{2\pi}$
	Quadratic	$\frac{1}{2}\sin\theta + \frac{1}{6}\sin 3\theta$	$\frac{\pi}{8}$	$\frac{\pi}{8}$	0	$\frac{1}{5}$	$\frac{8}{5\pi}$
	Cubic	$\frac{1}{\pi}\left[\cos^4\theta \log \tan\left(\frac{\pi}{4}+\frac{\theta}{2}\right) + \frac{7}{6}\sin\theta + \frac{1}{2}\cos 2\theta \sin\theta\right]$	$\frac{4}{15}$	$\frac{4}{15}$	0	$\frac{4}{9\pi}$	$\frac{5}{3\pi}$
	Quartic	$\frac{1}{4}\sin\theta + \frac{1}{8}\sin 3\theta + \frac{1}{40}\sin 5\theta$	$\frac{\pi}{16}$	$\frac{\pi}{16}$	0	$\frac{3}{28}$	$\frac{12}{7\pi}$
	Quintic	$\frac{1}{\pi}\left[\frac{2}{3}\cos^6\theta \log \tan\left(\frac{\pi}{4}+\frac{\theta}{2}\right) + \left(\frac{149}{180}+\frac{5}{9}\cos 2\theta + \frac{1}{12}\cos 4\theta\right)\sin\theta\right]$	$\frac{16}{105}$	$\frac{16}{105}$	0	$\frac{4}{15\pi}$	$\frac{7}{4\pi}$
Antisymmetric	Linear	$\frac{1}{2}\sin 2\theta$	0	$\frac{1}{3}$	$\frac{\pi}{32}$	$\frac{\pi}{16}$	$\frac{3\pi}{16}$
	Quadratic	$\frac{1}{\pi}\left[\frac{4}{3}\cos^3\theta \log \tan\left(\frac{\pi}{4}+\frac{\theta}{2}\right) + \frac{2}{3}\sin 2\theta\right]$	0	$\frac{2}{3\pi}$	$\frac{1}{15}$	$\frac{2}{15}$	$\frac{\pi}{5}$
	Cubic	$\frac{1}{4}\sin 2\theta + \frac{1}{16}\sin 4\theta$	0	$\frac{3}{20}$	$\frac{\pi}{64}$	$\frac{\pi}{32}$	$\frac{5\pi}{24}$
	Quartic	$\frac{1}{\pi}\left[\frac{4}{5}\cos^5\theta \log \tan\left(\frac{\pi}{4}+\frac{\theta}{2}\right) + \frac{17}{30}\sin 2\theta + \frac{1}{5}\cos 3\theta \sin\theta\right]$	0	$\frac{16}{45\pi}$	$\frac{4}{105}$	$\frac{8}{105}$	$\frac{3\pi}{14}$
	Quintic	$\frac{1}{96}(15\sin 2\theta + 6\sin 4\theta + \sin 6\theta)$	0	$\frac{5}{56}$	$\frac{5\pi}{512}$	$\frac{5\pi}{256}$	$\frac{7\pi}{32}$
	Flaps ($\theta_o = \cos^{-1} y_o^*$)	$\frac{2}{\pi}\left[(\pi - 2\theta_o)\sin\theta - (\cos\theta - \cos\theta_o)\log\frac{\sin\frac{\theta+\theta_o}{2}}{\sin\frac{\lvert\theta-\theta_o\rvert}{2}} - (\cos\theta+\cos\theta_o)\log\frac{\cos\frac{\theta+\theta_o}{2}}{\cos\frac{\theta-\theta_o}{2}}\right]$	$\left(\frac{\pi}{2}-\theta_o\right)+\frac{1}{2}\sin 2\theta_o$	$\left(\frac{\pi}{2}-\theta_o\right)+\frac{1}{2}\sin 2\theta_o$	0	(a)	$\frac{C_{BM}}{C_{L_{1/2}}}$
	Ailerons ($\theta_o = \cos^{-1} y_o^*$)	$\frac{2}{\pi}\left[(\cos\theta - \cos\theta_o)\log\frac{\sin\frac{\theta+\theta_o}{2}}{\sin\frac{\lvert\theta-\theta_o\rvert}{2}} - (\cos\theta+\cos\theta_o)\log\frac{\cos\frac{\theta+\theta_o}{2}}{\cos\frac{\theta-\theta_o}{2}}\right]$	0	(b)	$\frac{1}{8}\left(\sin\theta_o - \frac{1}{3}\sin 3\theta_o\right)$	$\frac{1}{4}\left(\sin\theta_o - \frac{1}{3}\sin 3\theta_o\right)$	$\frac{C_{BM}}{C_{L_{1/2}}}$

(a) $\frac{C_{BM}}{A\alpha} = \frac{1}{3}\left[2(\pi - 2\theta_o) - \left(\sin 2\theta_o - \frac{\sin 4\theta_o}{4}\right)\frac{1}{\sin\theta_o}\log\tan\left(\frac{\pi}{4}+\frac{\theta_o}{2}\right) + \sin 2\theta_o\right]$.

(b) $\frac{C_{L_{1/2}}}{A\alpha} = \frac{2}{\pi}\left[\sin\theta_o - \frac{1}{2}(\cos 2\theta_o + 2)\log\tan\left(\frac{\pi}{4}+\frac{\theta_o}{2}\right)\right]$.

NACA

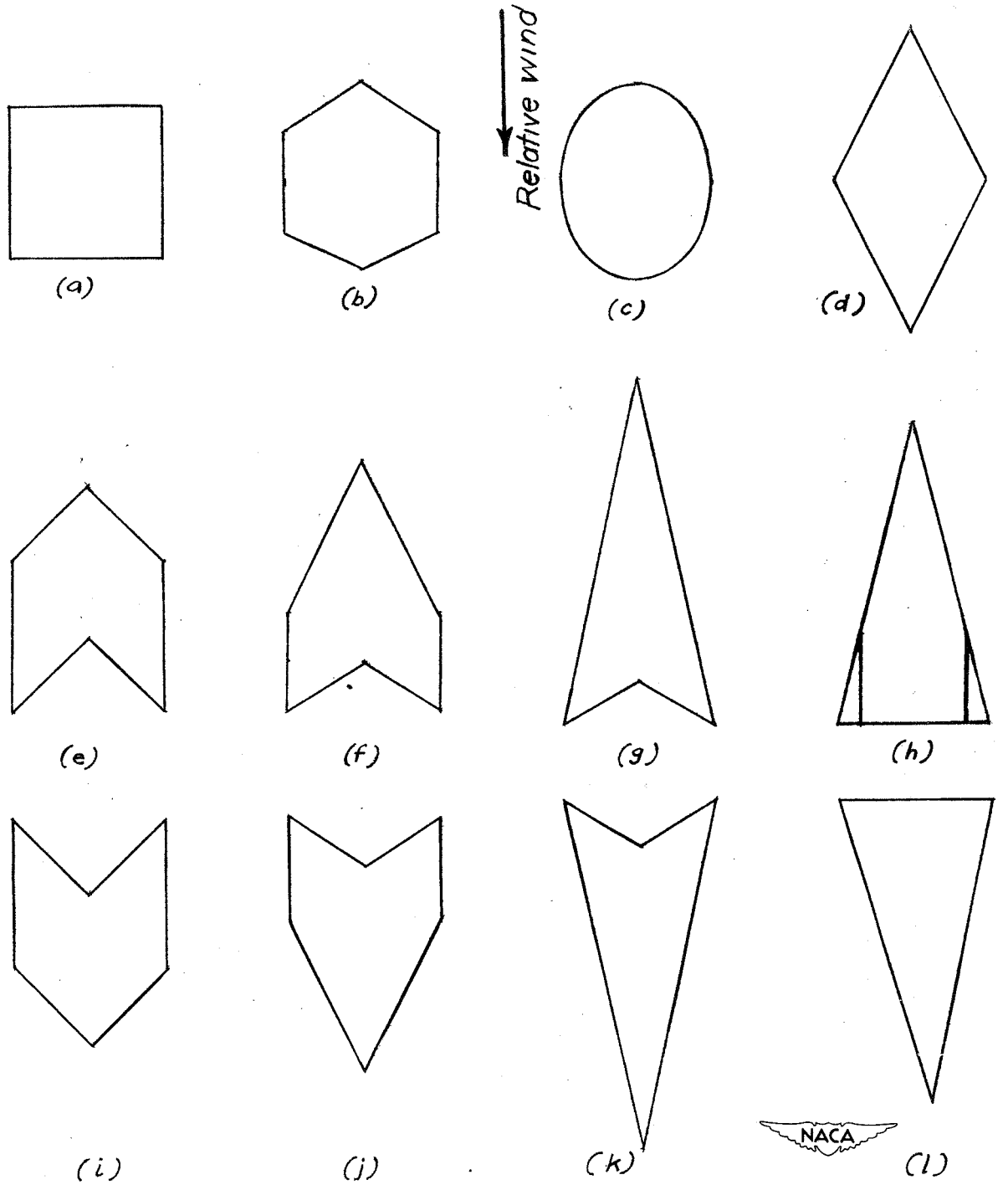

Figure 1.— Various plan forms of aspect ratio 1.

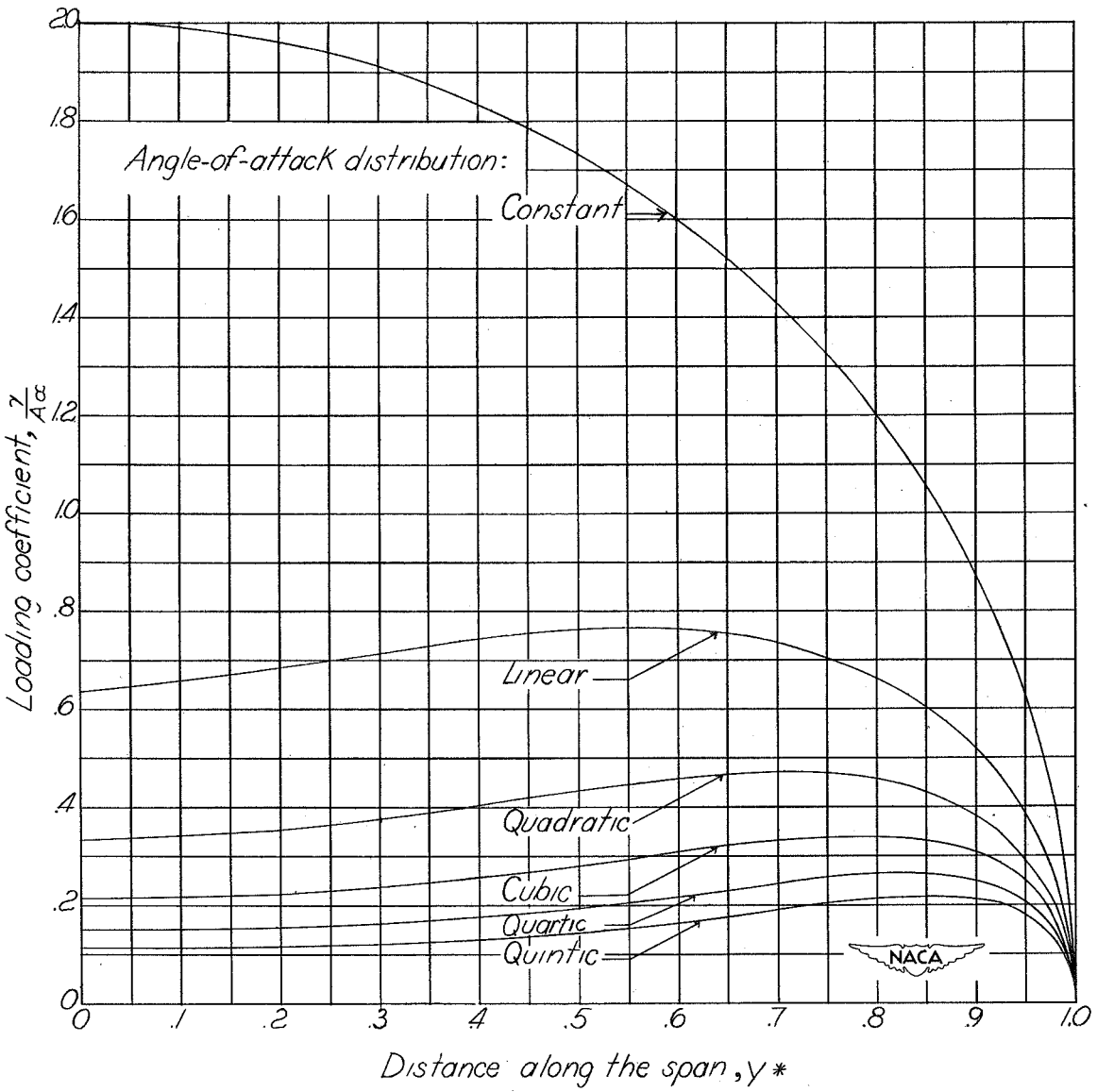

Figure 2.- Lift distribution of wings of low aspect ratio for constant angle of attack and for symmetrical twists.

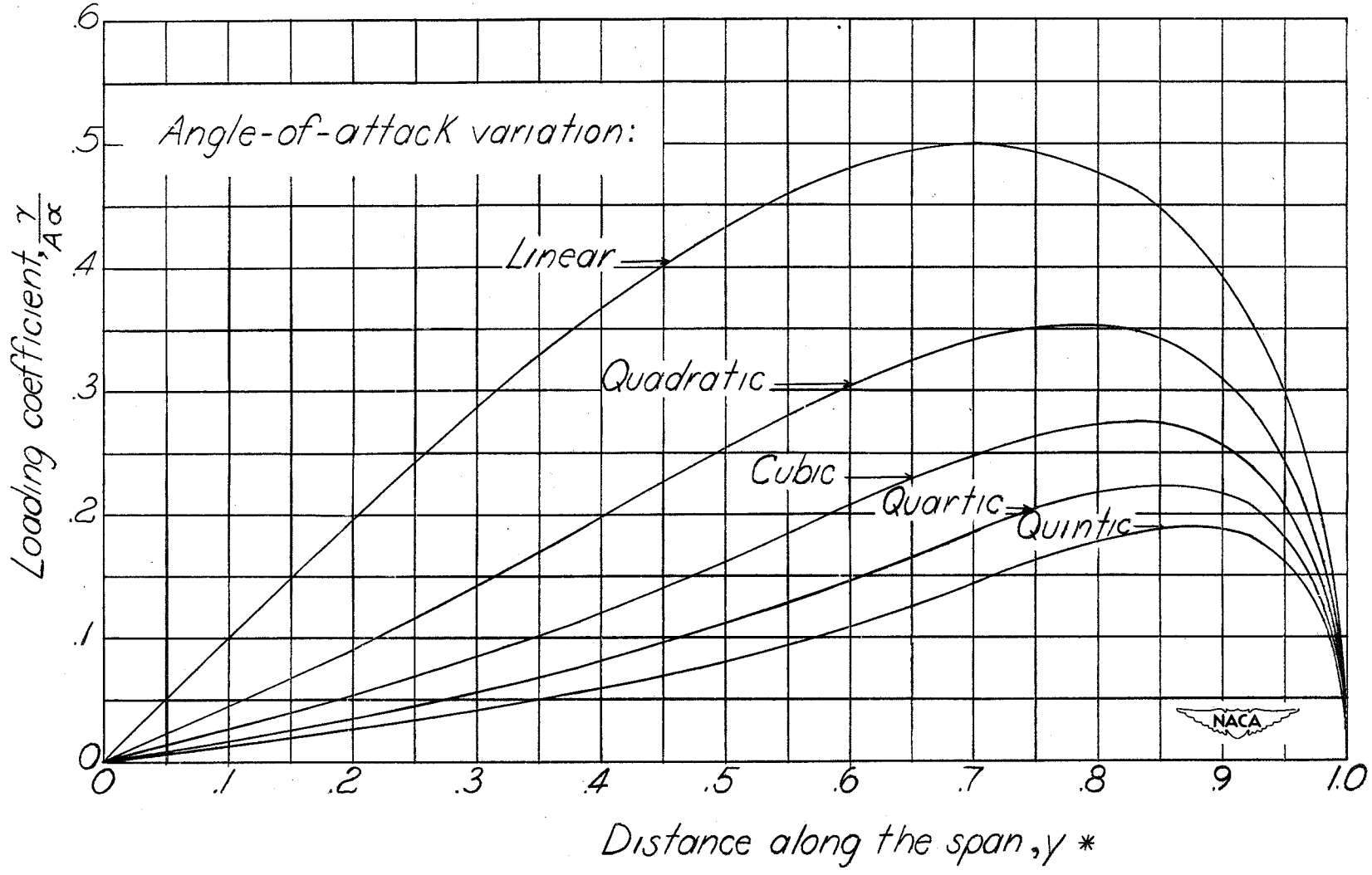

Figure 3.— Lift distributions of wings of low aspect ratio for antisymmetrical twists.

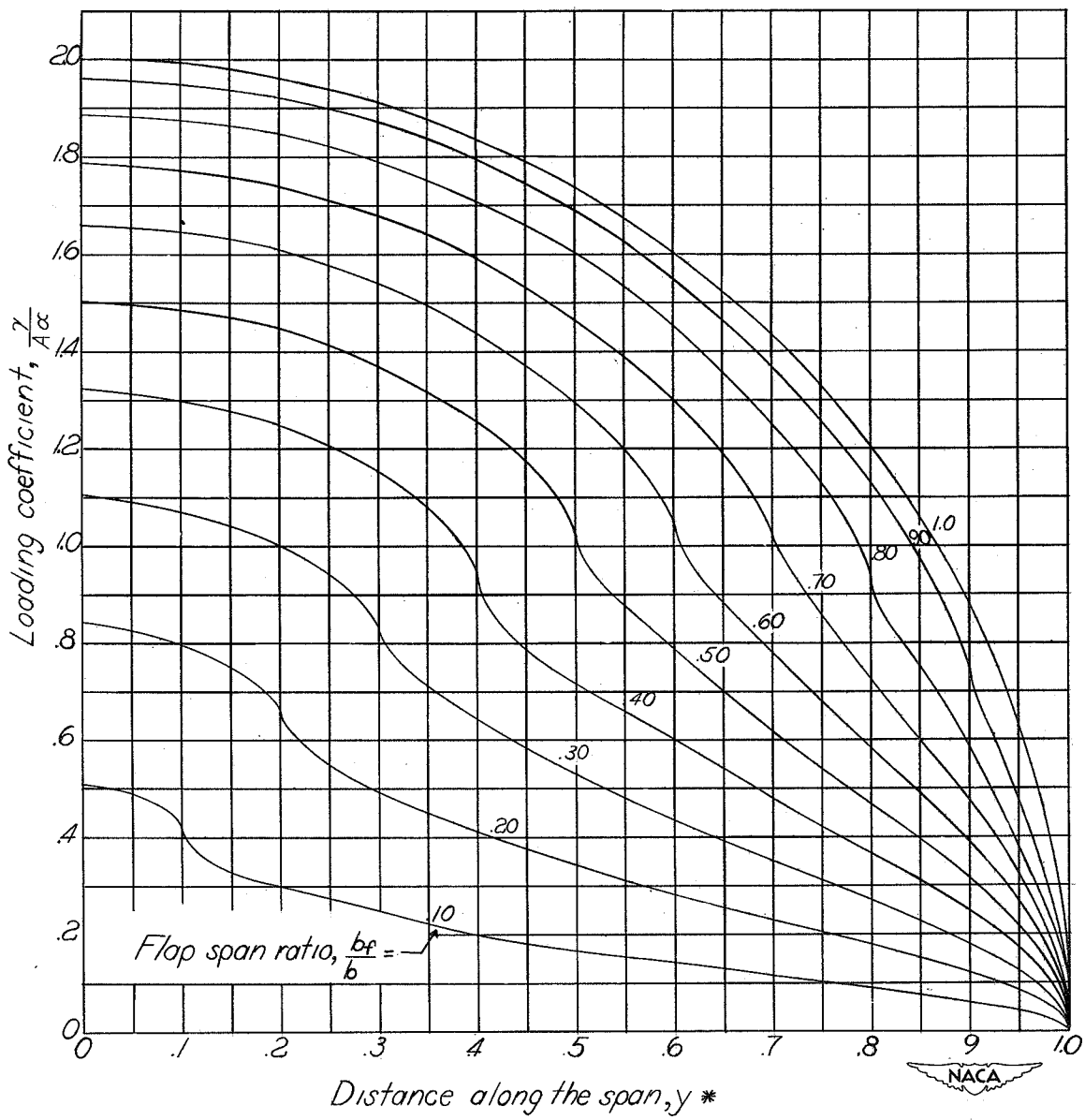

Figure 4.- Lift distributions of wings of low aspect ratio for flaps of various spans.

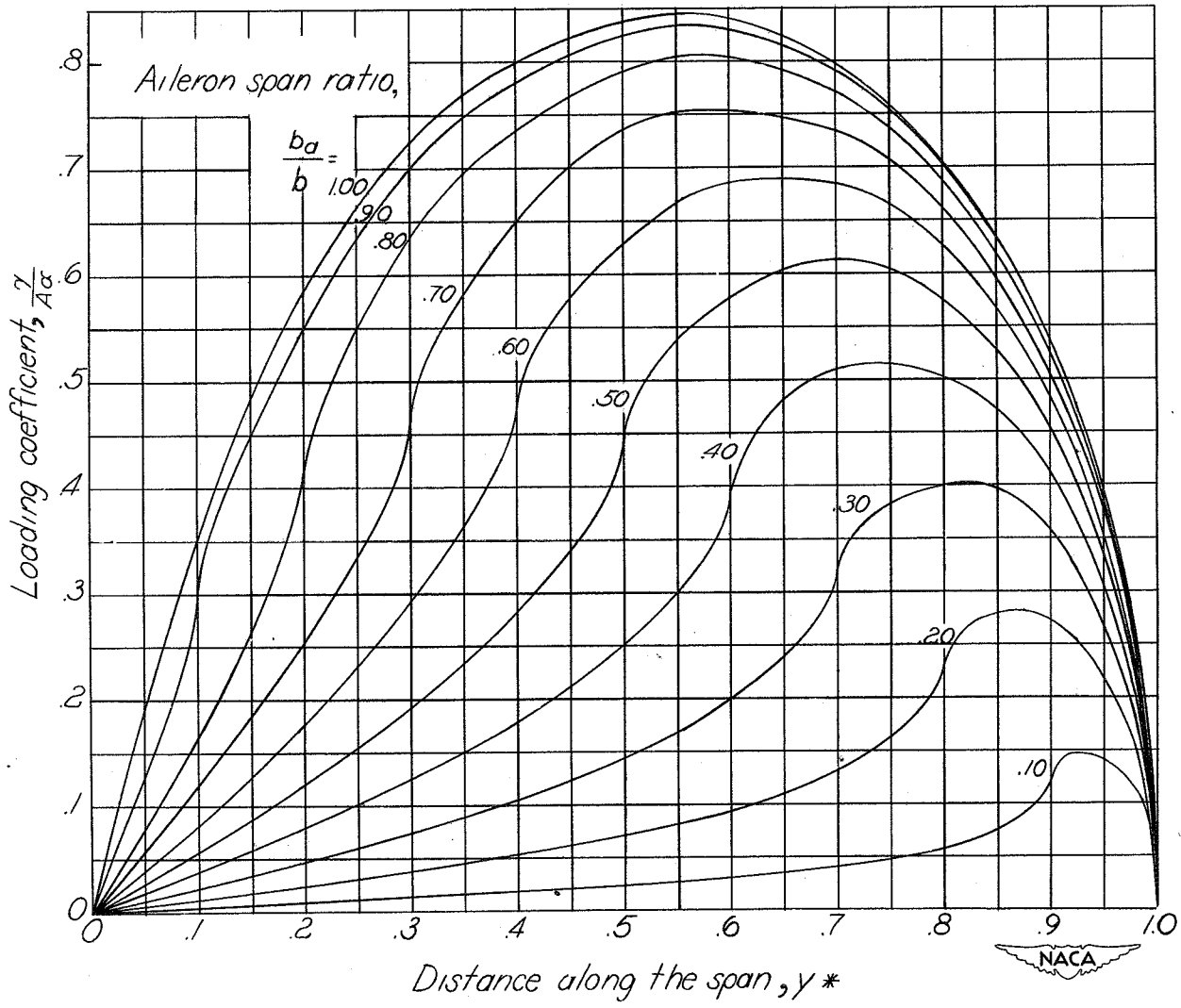

Figure 5.– Lift distributions of wings of low aspect ratio for ailerons of various spans.

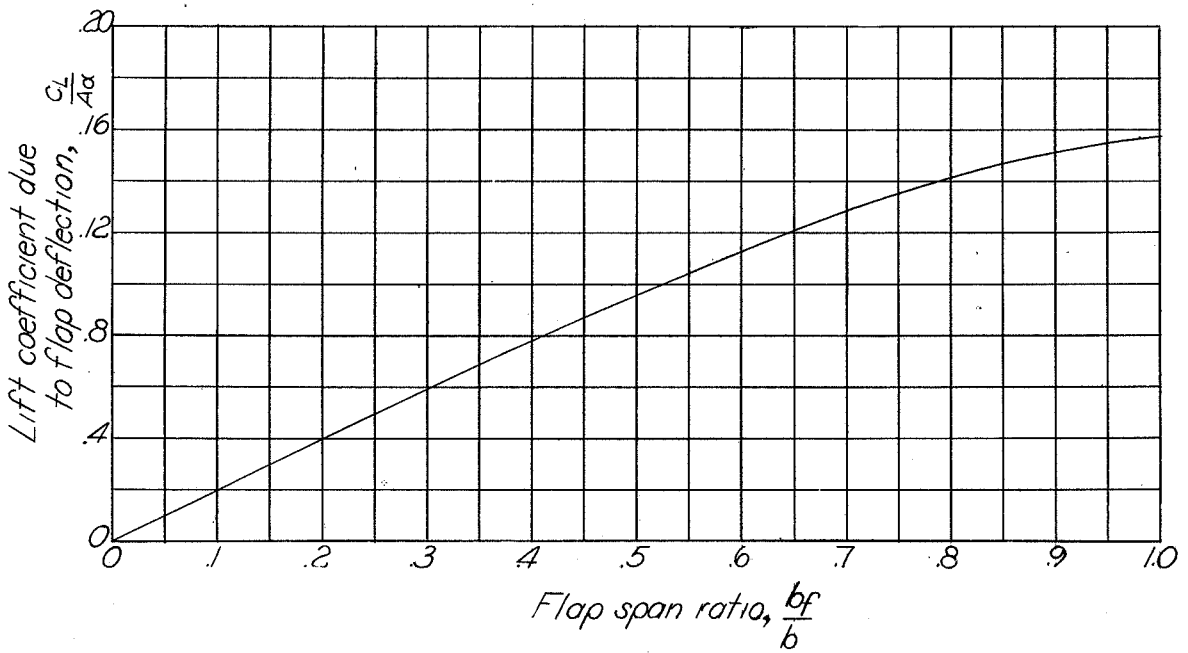

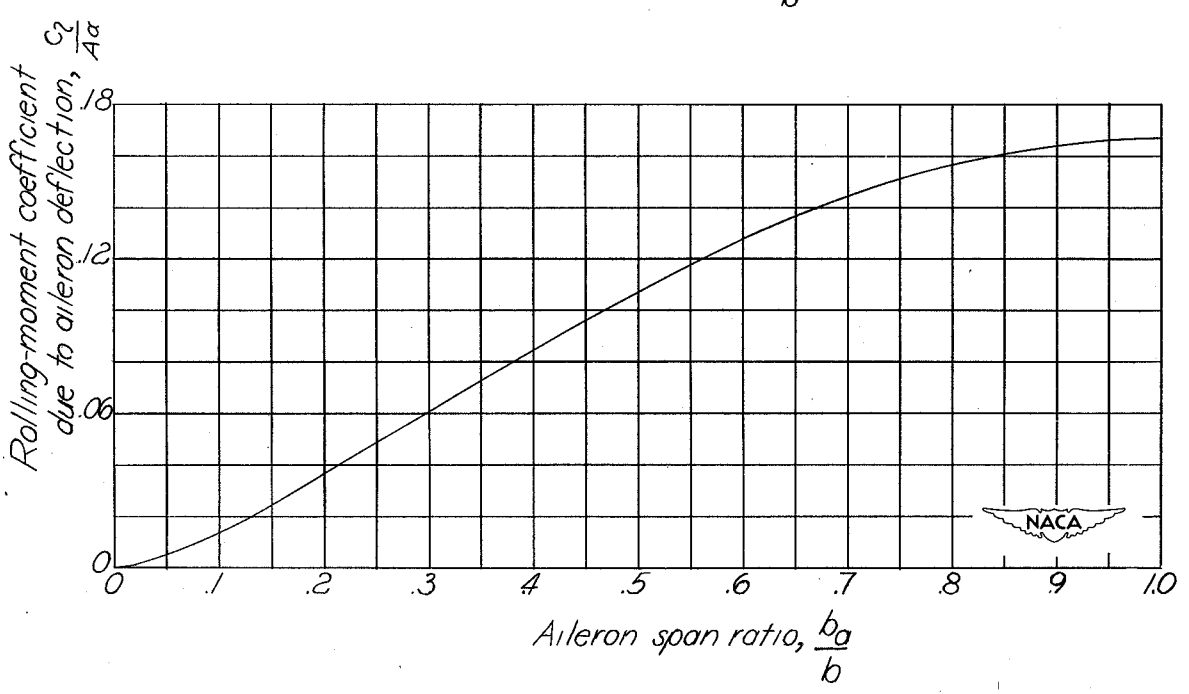

Figure 6.— Lift coefficient due to flap deflection and rolling-moment coefficients due to aileron deflections for wings of low aspect ratio.

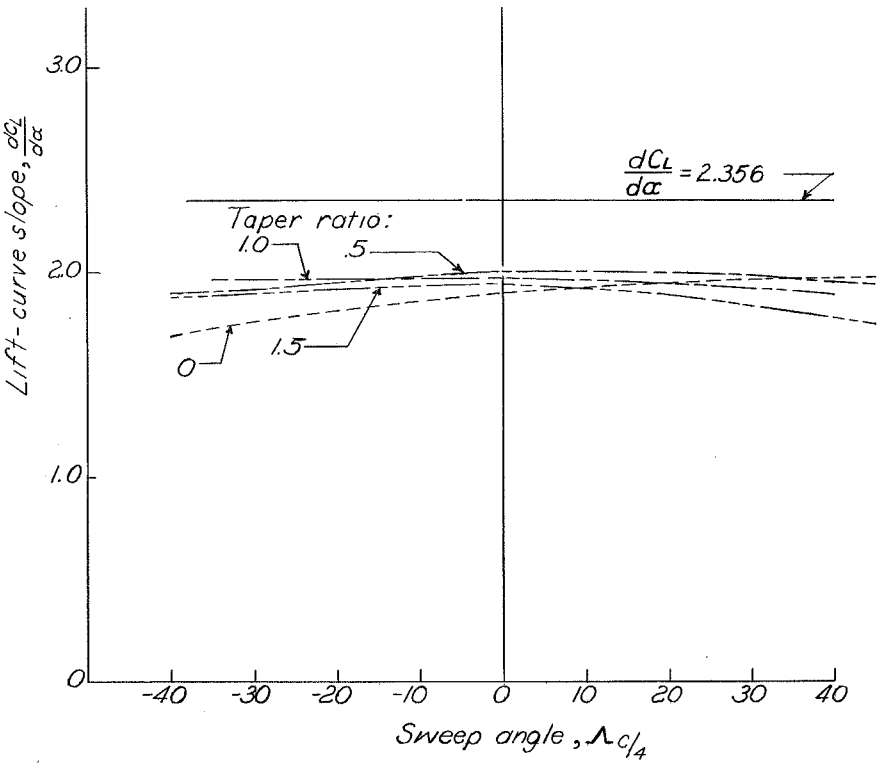

(a) Lift–curve slope.

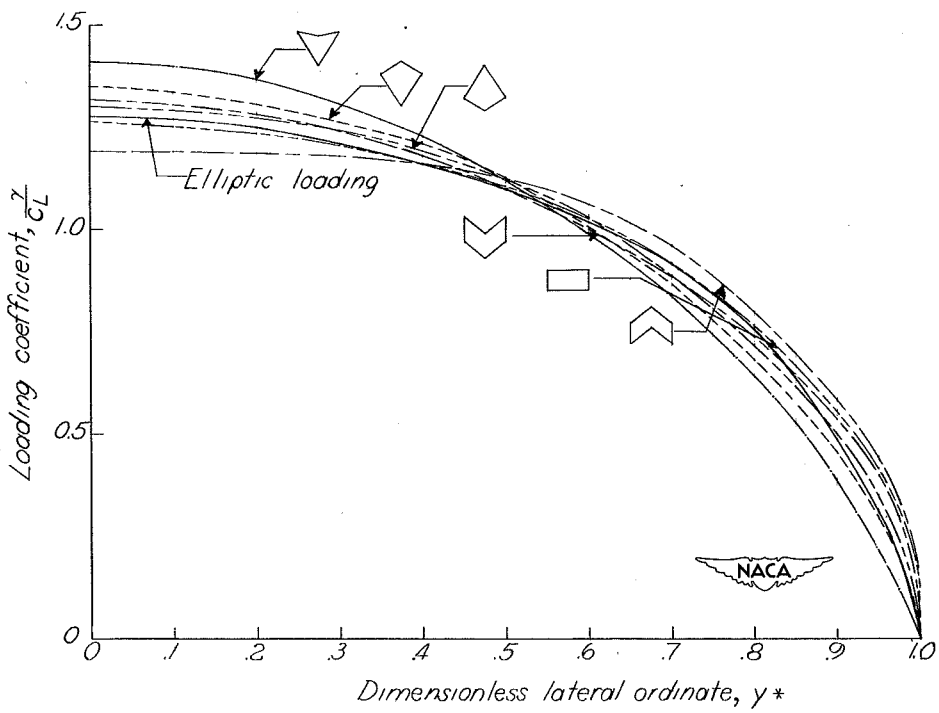

(b) Additional lift distributions.

Figure 7.– Comparison of results of low–aspect–ratio analysis and the Weissinger method for wings of aspect ratio 1.5.